

Examination of the Time–Water Content Superposition on the Dynamic Viscoelasticity of Moistened Polyamide 6 and Epoxy

A. Ishisaka, M. Kawagoe

Department of Mechanical Systems Engineering, Toyama Prefectural University, 5180 Kurokawa, Kosugi, Toyama 939-0398, Japan

Received 25 June 2003; accepted 15 January 2004

DOI 10.1002/app.20465

Published online in Wiley InterScience (www.interscience.wiley.com).

ABSTRACT: We have investigated the behavior of moisture absorption by the polyamide 6 and epoxy samples in various humid environments at constant temperature and also examined the effect of absorbed moisture on their dynamic viscoelastic properties. The moisture absorption was revealed to show the Fickian type of diffusion and to shift the dynamic viscoelastic properties of the specimen to those at lower temperature, as an effect of plasticization. Antiplasticization taken with an increase in the storage modulus was also observed in a low-temperature range below -50°C . The time–water content superposition was confirmed to

hold at various equilibrium water contents at constant temperature for both polyamide 6 and epoxy. The relation of the shift factor, $\log a_{T,H}$, to the equilibrium water content for polyamide 6 has a form similar to WLF equation of time–temperature superposition, whereas the $\log a_{T,H}$ for epoxy does not have such a form. © 2004 Wiley Periodicals, Inc. *J Appl Polym Sci* 93: 560–567, 2004

Key words: polyamides; resins; diffusion; viscoelastic properties; glass transition

INTRODUCTION

The polymeric materials are used in a wide variety of fields for their several surpassing properties. The mechanical properties of polymers are, however, strongly influenced by various environmental factors. Water penetrating into polymers especially reduces their mechanical performance by some mechanisms such as a plasticization effect. Thus, it is important to accurately examine the effect of absorbed water on the mechanical properties of polymeric materials. In addition, it may be beneficial to predict a long-term mechanical behavior of polymers under the water environment for applying the polymers and polymer-based composites to the structural components, for which the durability is strongly required.

One of the principles for estimating the long-term behavior of polymers may be a time–temperature superposition (equivalence), based on the viscoelastic properties of polymers varying with time and temperature. By this principle, one may predict the long-term properties from the short-term data at various temperatures. The viscoelasticity of polymers depends not only on temperature but also on the absorbed moisture. It generally brings about reductions in the glass

transition temperature and the storage modulus. With regard to the reduction in the modulus with increasing water content, the effect of moisture is supposed to be equivalent to that of temperature. Therefore, an alternative principle of superposition exchanging the temperature for the water content may be suggested.

Past studies^{1–4} of the effects of moisture on the viscoelastic behavior of polymers have showed that a master curve may be constructed from the short-term viscoelastic data at various water contents at a fixed temperature. That is, the absorbed water in polymers has an analogous effect to temperature, and thus, a so-called time–water content (moisture) superposition may hold. This kind of superposition is expected to predict the long-term variations in the mechanical properties of polymeric materials under the water environments. However, the studies of time–water content equivalence have so far been restricted to a few kinds of thermoplastic polymers only under the static loading (creep,^{1,3} stress relaxation^{2,4}). Thus, this principle on the equivalence between time and water content remains to be satisfactorily confirmed, especially on the dynamic viscoelasticity and for other polymeric materials (e.g., thermosetting polymers, fiber-reinforced polymers).

We have previously investigated the effects of moisture on the dynamic viscoelastic behavior of epoxy resin, a typical thermosetting polymer, and examined the time–water content superposition for the saturated

Correspondence to: M. Kawagoe (kawagoe@pu-toyama.ac.jp).

samples at various humidities at 60°C.⁵ Because the viscoelastic factor (storage modulus) showed only a small change with the water content, the examination of this superposition was inadequate. Thus, for aiming to demonstrate the time–water content equivalence, it may be proper to chose a model polymer with great ability of moisture absorption such as polyamide (PA).

The purpose of this study is to evaluate such a hydroeffect of absorbed moisture on the dynamic viscoelastic properties of polyamide 6 (PA6), which is prepared in an environment where the humidity in air is controlled independently of temperature, with particular reference to the time–water content superposition. For comparison, the hydroeffect on the dynamic viscoelasticity of epoxy resin (EP) is also reexamined in detail for confirmation of the above superposition to hold, although EP resin has less ability of moisture absorption.

EXPERIMENTAL

Materials

PA6 (Ube Co. Ltd., Japan; Ube Nylon6 S1013NW8) and epoxy resin (Cape2002) were used for this study, because of their hydrophilic property, especially for PA6, which was appropriate to the examinations of the hydroeffects of absorbed moisture on the viscoelastic behavior.

The PA6 pellets were preliminarily dried at 80°C for 3 h in a vacuum chamber (Shibata Scientific Technology Ltd., Japan; VOR-300) and then uniformly dispersed in a rectangular mold of stainless steel. The pellets in the mold were heated at 225°C for 5 min and then compressed under about 15 MPa for 5 min by means of hot-pressing equipment (Imoto Co. Ltd., Japan; TF1) to make a PA6 sheet of 2 mm thickness. In this study, PA 6 is used as a model polymer to more clearly grasp the hydroeffect on the dynamic viscoelastic behavior through greater moisture absorption. For this purpose, in addition, the PA sheet was quenched from that temperature into water at 15°C for introducing a lower degree of crystallization; in other words, a higher content of amorphous phase that may absorb and store the water. However, the quenched PA6 may give rise to some variations in microstructure similar to crystallization of amorphous phase followed by water absorption. Although this problem is not discussed here, it is now planned to be examined in the near future, because of its significance for understanding a long-term mechanical behavior of PA specimen. The degree of crystallization of PA6 sheet was calculated from the equation⁶:

$$X(\%) = \frac{\rho_c(\rho - \rho_a)}{\rho(\rho_c - \rho_a)} \times 100 \quad (1)$$

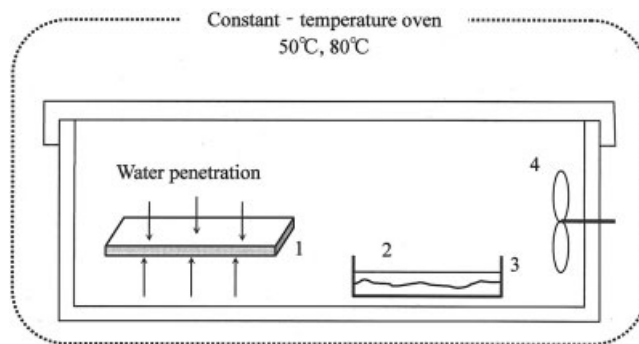


Figure 1 Schematic of moisture absorption test (1: specimen; 2: salt solution; 3: petri dish; 4: fan).

where ρ_c , ρ_a , and ρ are the densities of the crystal phase (1.23 g/cm³),⁷ amorphous phase (1.10 g/cm³),⁷ and whole specimen, respectively. The density of the PA6 sheet was measured by an electronic densimeter (Mirage Co. Ltd., Japan; SD-200L) based on the Archimedes method (JIS K7112⁸). The degree of crystallization calculated by eq. (1) was about 25%.

The epoxy resin in liquid state was put into a mold on the hot-pressing device and then heated at 60°C for 1 h and subsequently at 127°C for 1 h. After curing by heating, the epoxy sheet was slowly cooled to room temperature. This procedure of sample preparation was performed at the Kanazawa Institute of Technology and Stanford University. The surfaces of the epoxy sheet were flatly machined to eliminate, as much as possible, small cavities that were formed and gathered mainly on the surface layers during the heating process. The sheet was finally adjusted to have a thickness of 1.5 mm.

The specimens of PA6 and epoxy were cut from each sheet to the dimensions of 80 × 10 mm. All the specimens were predried in a vacuum oven (Shibata Scientific Technology Ltd., VOR-300) at 100°C for 3 h and then slowly cooled to room temperature. The cut sides of predried specimens were coated with a silicone adhesive for protection from water penetration.

Moisture absorption test

The moisture absorption test was done in various humid environments at constant temperature. We used a saturated salt solutions method⁹ to make various relative humidities. Five kinds of salt (MgCl₂, NaBr, NaNO₃, KCl, and K₂SO₄) for the environment of each relative humidity were put into the closed vessels to make the saturated salt solutions. The schematic of test equipment and the relative humidity (RH) obtained in this way are shown in Figure 1 and Table I, respectively. All the vessels were kept in an oven at constant temperatures (50 and 80°C). The air in each vessel was stirred by a fan to make uniform RH and

TABLE I
Relative Humidity Given by a Method with Saturated Salt Solutions

	MgCl ₂	NaBr	NaNO ₃	KCl	K ₂ SO ₄
50°C	29% RH	48% RH	65% RH	77% RH	92% RH
80°C	—	44% RH	55% RH	69% RH	85% RH

temperature. The absorbed moisture in the specimen was measured by weighing the specimen by using an electronic analytical balance (Mettler-Toledo, Switzerland; AE-240) with a resolution of 0.01 mg. The water content, M_t , was determined by:

$$M_t(\text{wt } \%) = \frac{W_t - W_0}{W_0} \times 100 \quad (2)$$

where W_t and W_0 are the weights of wet specimen at exposure time, t , and of the dried specimen after predrying, respectively.

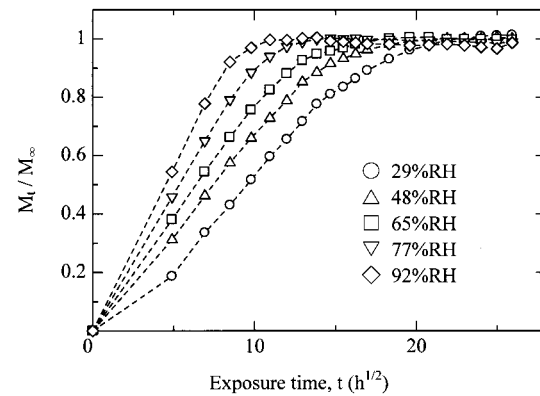
Dynamic viscoelastic test and examination of time-water content superposition

The dynamic viscoelastic behavior was evaluated by a dynamic viscoelastic analyzer (Orientec Co. Ltd., Japan; VFA-1KNA). The test conditions are shown in Table II. The storage modulus (E'), loss modulus (E''), and loss tangent ($\tan \delta$) were measured as a function of temperature. Before the test, the moistened samples were weighed, and then the gauge surfaces were coated with silicone adhesive for preventing water from desorption. The effects of surface coating on the viscoelastic properties were preliminarily examined on the temperature dependence of viscoelasticity of dried specimens, by comparing with the specimens without surface coating. According to these preliminary experiments, no influence of surface coating on the viscoelasticity was observed, except for a small and sharp $\tan \delta$ peak at about -128°C due to the silicone adhesive.

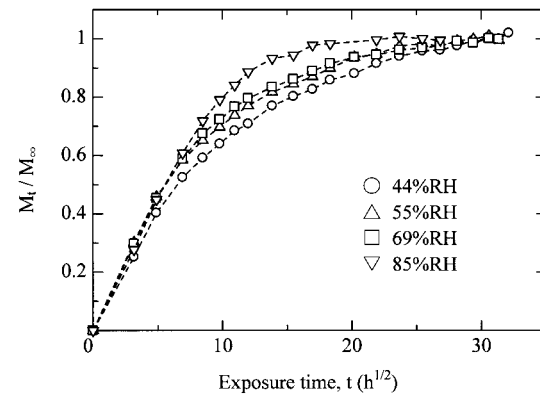
The time-water content superposition was examined by using the moistened specimens, in which the water content reached the equilibrium value, M_∞ , in each exposure environment. The frequency depen-

TABLE II
Conditions of Viscoelastic Tests

Test mode	Temperature dependence	Frequency dependence
Temperature range	-150 to 200°C	Constant
Heating rate	$2^\circ\text{C}/\text{min}$	—
Static pre-tension		14.7N
Amplitude		25 μm
Frequency	1.0 Hz	0.1–30 Hz



(a) Polyamide 6 at 50°C



(b) Epoxy at 80°C

Figure 2 Moisture absorption behavior of polyamide 6 and epoxy.

dence of E' was also evaluated by the dynamic viscoelastic analyzer at the same temperature as for the moisture absorption test (Table II) to obtain a relation of E' to time, which was given by a reciprocal applied frequency. Shifting the curves of E' along the logarithmic scale of time for a reference water content, M_0 , may give a master curve describing the time-water content superposition.

RESULTS AND DISCUSSION

Moisture absorption behavior

The moisture absorption behavior by PA6 and EP is shown in Figure 2. The water content, M_t , is rapidly increased at an early stage of absorption and gradually reaches the equilibrium value, M_∞ . The ratio of M_t/M_∞ linearly increases with the square root of soaking time, $t^{1/2}$, and the gradient of M_t/M_∞ versus $t^{1/2}$ curve increases with RH in the environment. The water absorption behavior by PA6 and EP thus may be expressed by the Fickian equation of diffusion, and consequently, the moisture uptake and diffusion pro-

TABLE III
Equilibrium Water Content and the Diffusion Coefficient of Water

Salt	Polyamide 6 (50°C)		Epoxy (80°C)	
	M_∞ (wt %)	D (mm ² /h)	M_∞ (wt %)	D (mm ² /h)
MgCl ₂	0.88	3.15×10^{-3}	—	—
NaBr	1.95	3.65×10^{-3}	1.18	2.86×10^{-3}
NaNO ₃	3.18	4.30×10^{-3}	1.64	3.79×10^{-3}
KCl	4.63	5.98×10^{-3}	2.45	3.52×10^{-3}
K ₂ SO ₄	6.78	9.33×10^{-3}	3.53	3.90×10^{-3}

cess described by the following equation at the early absorption stage¹⁰:

$$\frac{M_t}{M_\infty} = \frac{4}{\pi^{1/2}} \left(\frac{Dt}{h^2} \right)^{1/2} \quad (3)$$

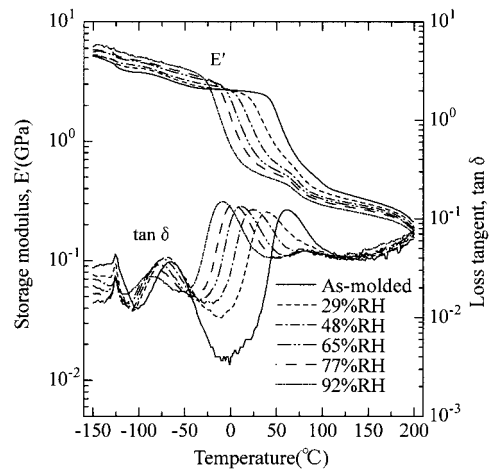
The diffusion coefficient is obtained by eq. (4) from the initial gradient of the absorption curve:

$$D = \frac{\pi}{16} (k \times h)^2 \quad (4)$$

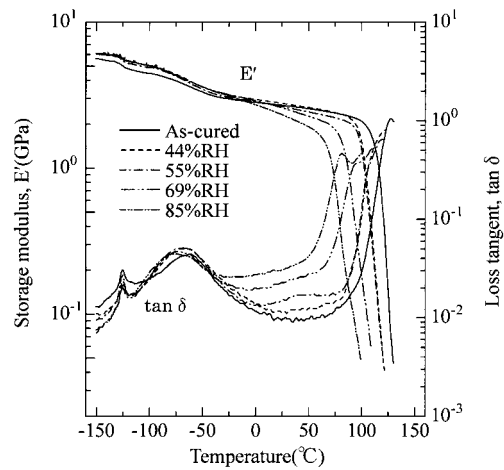
where D is the diffusion coefficient, k is the initial gradient of M_t/M_∞ versus $t^{1/2}$ plot, and h is the initial thickness of sheet specimen. The equilibrium water content and the diffusion coefficient are summarized in Table III. The value of M_∞ is clearly dependent on the moisture concentration in the exposure environment. The diffusion coefficient of EP is not so dependent on the moisture concentration, whereas that of PA6 strongly depends on the moisture concentration.

Influence of absorbed moisture on the dynamic viscoelastic behavior

The influence of absorbed moisture on the temperature dependence of dynamic viscoelasticity of PA6 is shown in Figure 3(a). The as-molded PA6 sample (solid line) shows three peaks of $\tan \delta$ at approximately -135 , -65 , and 60°C , which are known as the γ -, β -, and α -relaxations, respectively.⁶ The α -relaxation is brought about by the long-chain segmental motion in the amorphous region, as a result of rupture of hydrogen bonds between the polymer chains (i.e., the glass transition of PA6). The β -relaxation arises from the motion of nonbonded amide groups in the amorphous region. The γ -relaxation is due to the segmental motion in the amorphous region with a small number of methylene groups between the amide groups. After the moisture absorption, the peak of α -relaxation shifts to a lower temperature with increasing water content. This may mean that water molecules penetrate into the spaces between the mo-



(a) Polyamide 6



(b) Epoxy resin

Figure 3 Temperature dependences of viscoelastic properties of polyamide 6 and epoxy after moisture absorption.

lecular chains and facilitate the segmental motion in the amorphous region (i.e., a plasticization effect). Figure 4 shows the reduction in glass transition temperature, T_g , given by the α -relaxation peak temperature

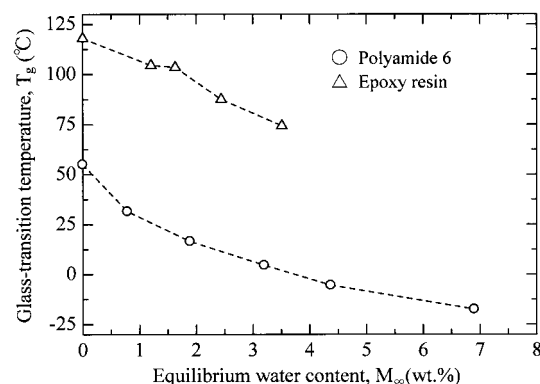


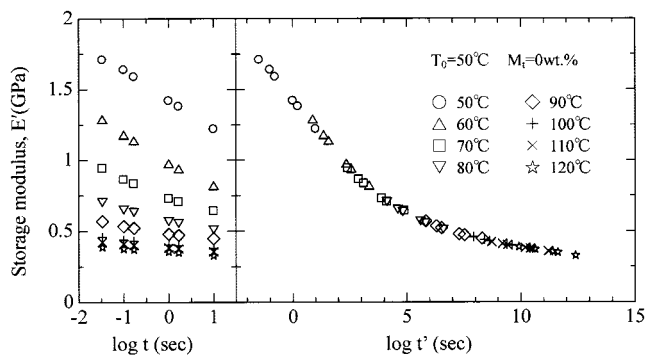
Figure 4 Reduction in T_g against the equilibrium water content.

of E'' measured by the dynamic viscoelastic analysis at 1 Hz. The T_g of PA6 is decreased by 20 to 70°C. In the low-temperature region below 0°C, both β - and γ -relaxation peaks decrease with increasing water content. It may result from the bridges formed between the water molecule and the amide group of PA, ¹¹ which restrains the molecular motion. Therefore, the E' of the moistened samples is higher than that of an as-molded one in low-temperature region (i.e., an anti-plasticization).

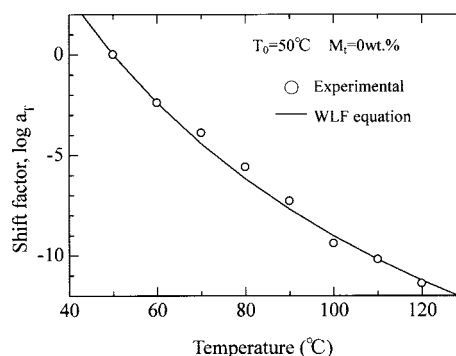
The temperature dependence of viscoelasticity of EP specimens treated by the moisture absorption is shown in Figure 3(b). In general, the $\tan \delta$ curves for the as-cured EP (solid line) exhibit two major peaks.^{12,13} One $\tan \delta$ peak at a higher temperature (about 125°C) corresponds to the glass transition of EP, which occurs by micro-Brownian motion of main chain. The other at a lower temperature (about -60°C) may be interpreted as a result of local segmental motion. By the moisture absorption treatment, the α -relaxation shifts to a lower temperature region with increasing water content as a result of plasticization, leading to a reduction in T_g by 15 to 50°C. In addition, the height of the α -relaxation peak is decreased with a broadening of the spectrum, and an alternative peak newly appears with increasing water content. The similar phenomena were observed in the other studies.^{14,15} Such a splitting of $\tan \delta$ peak is supposed as the result of a differential plasticization state in α -relaxation,¹⁴ being caused by coexistence of a micro-structural plasticized region by the moisture and nor or less-plasticized one. Because the surface coating with silicone adhesive does not provide any influence on the $\tan \delta$ behavior in this higher temperature region, as previously stated, and seems to sufficiently suppress the drying of moistened specimen during the heating process of dynamic viscoelastic test, the above phenomenon of splitting of the $\tan \delta$ peak in α -relaxation probably may occur by the above differential plasticization mechanism, although some detailed examinations for confirming the water desorption during the test may be required for more strict discussion. In the low-temperature region (<0°C), E' of moistened samples are higher than that of the as-cured EP sample. However, the anti-plasticization and the plasticization effects of moisture on the β -relaxation are not clearly observed, being different from PA6.

Examination of time–water content superposition

Prior to the investigation of time–water content superposition (TWS), the applications of time–temperature superposition (TTS) to PA6 and EP are examined. Figures 5 and 6 show the results of examination for the storage modulus E' of as-molded PA6 and as-cured EP specimens, respectively, which were measured at various temperatures. Shifting E' at each temperature



(a) Master curve



(b) Shift factor $\log [a_T]$

Figure 5 Application of time–temperature superposition to the as-molded polyamide 6 specimen.

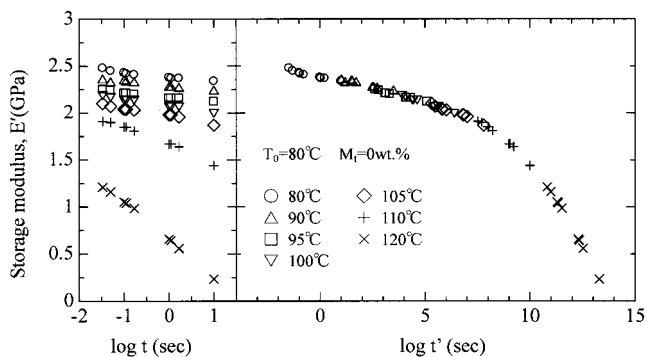
as to a reference temperature, T_0 , gives a smooth master curve. The temperature dependence of shift factor, $\log a_T$, is generally represented by the following two equations below and above T_g , respectively¹⁶:

$$\log a_T = \frac{\Delta H}{2.303R} \left(\frac{1}{T} - \frac{1}{T_0} \right) \quad (\text{Arrhenius-type equation}) \quad (5)$$

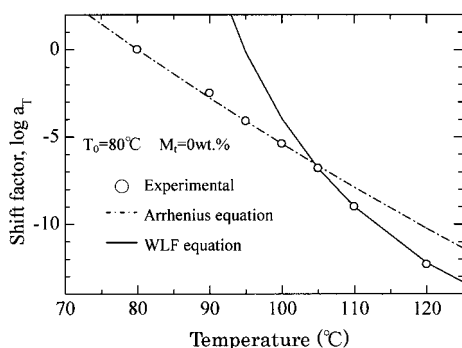
and

$$\log a_T = -\frac{C_1(T - T_0)}{C_2 + T - T_0} \quad (\text{WLF-type equation}) \quad (6)$$

where T_0 is the reference temperature, ΔH is the activation energy, R is the gas constant, and C_1 , C_2 are the experimental constants, respectively. In this study, because the T_g 's of PA6 and EP specimens are about 55 and 118°C (Fig. 4), respectively, the temperature dependence of $\log a_T$ may be described by WLF-type equation for PA6, and by Arrhenius- and WLF-type equations for the EP specimen. The relationship be-



(a) Master curve



(b) Shift factor $\log [a_T]$

Figure 6 Application of time–temperature superposition to the as-cured epoxy specimen.

tween $\log a_T$ and temperature are shown in Figures 5(b) and 6(b). The lines in each figure show the calculated value by the above equations. The behavior of PA6 shows good agreement with the WLF-type equation. For EP, one also may find that the tendency of $\log a_T$ for the temperature changes from WLF-type to Arrhenius-type equations near the glass transition region with decreasing temperature.

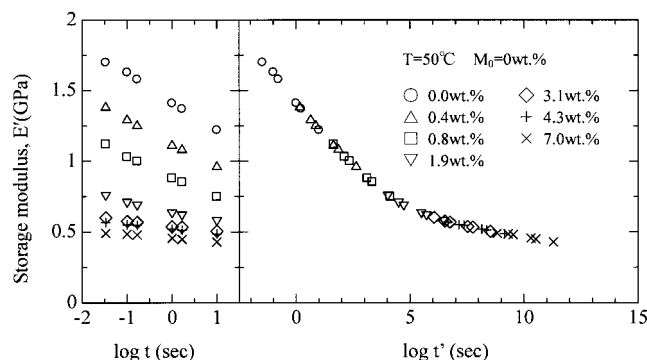
Next, the application of time–water content superposition is examined. Figures 7 and 8 show the results of examination for the moistened PA6 and EP specimens, respectively. The left side of each upper figure (a) shows the variation of E' with time at various equilibrium water contents, M_∞ . The low water concentration (0.4 wt %) in the PA6 sample was adjusted by leaving the sample in air at 29% RH. These figures clearly show that the E' is decreased with increasing water content. Thus, the effect of increasing water content on the E' may be equivalent to that of rising temperature. We chose here M_0 of 0 wt % as a reference water content to directly compare the master curve of TWS with that of TTS for the dried sample. The master curves were constructed by shifting E' at each M_∞ along the logarithmic scale of time as to a

reference water content, M_0 of 0 wt %. They overlap each other to form a single smooth curve, as shown in the right side of figure. The master curves of TWS on both polymers are very similar to those of TTS, as shown in Figures 5 and 6. Thus, it is demonstrated that the time–water content superposition holds for both PA6 and EP.

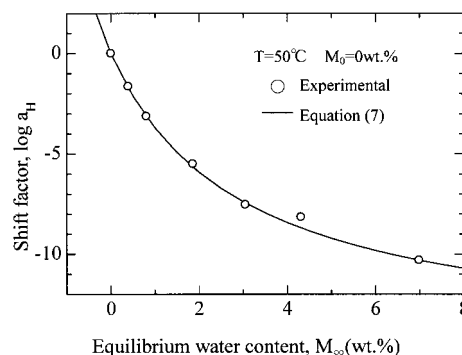
The shift factors on this hygroeffect, $\log a_{H'}$, of PA6 and EP specimens are plotted in Figures 7(b) and 8(b), respectively. The relationship between $\log a_{H'}$ and the equilibrium water content is analogically described by the WLF-type equation [eq. (6)] on the time–temperature superposition^{1,3}:

$$\log a_H = -\frac{D_1(M - M_0)}{D_2 + M - M_0} \tag{7}$$

where M is a water content at time, t , M_0 is a reference water content, and D_1 , D_2 are the empirical constants determined by the experiment. For PA6, the solid line in Figure 7(b) shows the result calculated from eq. (7) with the values of D_1 and D_2 equaling 14.66 and 2.96 wt %, respectively. The figure shows good agreement

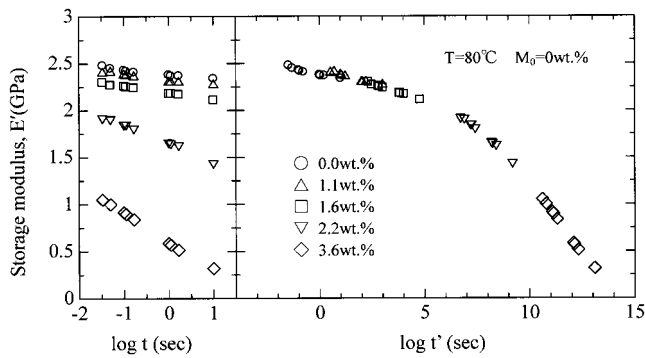


(a) Master curve



(b) Shift factor $\log [a_{H'}]$

Figure 7 Application of time–water content superposition to polyamide 6 at 50°C.



(a) Master curve

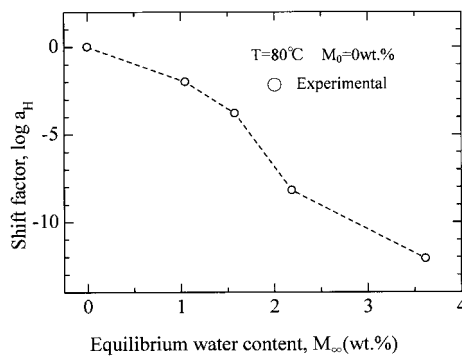
(b) Shift factor $\log [a_H]$

Figure 8 Application of time–water content superposition to epoxy at 80°C.

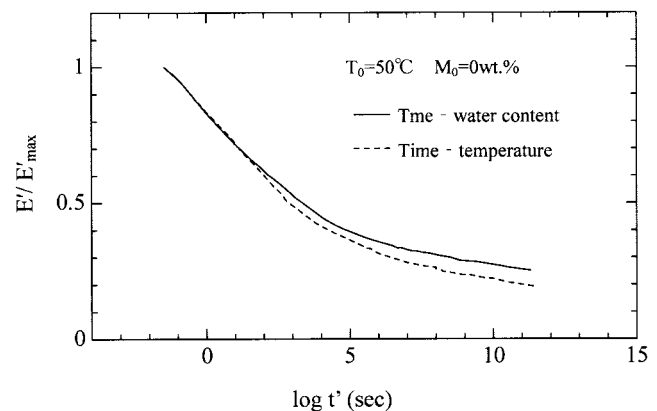
with the experimental data. On the other hand, for EP specimen, the $\log a_H$ may not be satisfactorily expressed by eq. (7). Considering the similar effects between temperature and moisture, this consequence may result from the finding that the T_g of epoxy is not significantly lowered below the environmental temperature even after the moisture absorption. Thus, it may be necessary to apply another expression of $\log a_H$ to water content, such as the Arrhenius-type equation for the time–temperature superposition below T_g . Therefore, in order to strictly confirm the time–water content superposition, it is required to examine at much wider range of water content.

For the same reference temperature and the water content, the master curve obtained by TWS should be completely overlapped to that given by TTS. The comparison of the master curve of TWS with TTS is shown in Figure 9. In current studies,^{2,3} both TWS and TTS of some hydrophilic polymers are shown to have the master curves of TWS and TTS, which are overlapped with each other for the same reference temperature and water content. In this study, although they are in accordance with each other for a short-term region, the master curve of TWS is slightly different from that

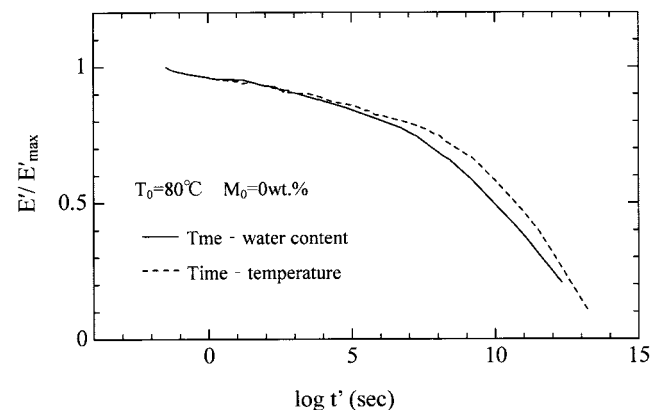
of TTS for a long-term region. The master curve of TWS on PA6 is generally higher than that of TTS, whereas that of TWS on EP specimen is lower than that of TTS. Such a difference between TWS and TTS may be caused by some structural changes of material during the moisture absorption. In the case of PA6, for example, an increase in E' is due to an increase in the degree of crystallinity by the moisture, and that in epoxy may be given some degradation by hot and wet conditions.

CONCLUSION

In this work, we have investigated the behavior of moisture absorption by polyamide 6 and epoxy resin, which were stored in various humidities at constant temperature. In addition, the effects of moisture on the dynamic



(a) Polyamide 6



(b) Epoxy resin

Figure 9 Comparison of master curve obtained by time–water content superposition with that by time–temperature superposition.

viscoelastic properties were also examined with particular reference to the time–water content superposition. The moisture absorption behavior of polyamide 6 and epoxy resin was revealed to show the Fickian diffusion. For the dynamic viscoelastic behavior, the absorbed moisture generally gave rise to a plasticization, while in a low-temperature region ($<0^{\circ}\text{C}$), the absorbed moisture resulted in an anti-plasticization phenomenon showing an increase in the storage modulus. The time–water content superposition was demonstrated to hold for both the polyamide 6 and the epoxy samples. For polyamide 6, the relationship between the shift factor, $\log a_{HT}$, and equilibrium water content, M_{∞} , was shown to be similar to the WLF-type equation of time–temperature superposition, whereas for epoxy, the relation gave a different expression. In addition, the master curve of time–water content superposition did not completely agree with that of time–temperature superposition observed in this study. The discrepancy may be due to some structural changes of material caused by the absorbed water.

The authors thank Professor Y. Miyano and N. Sekine, Kanazawa Institute of Technology, and Professor S. W. Tsai and A. Kuraishi, Stanford University, for preparing and supplying the epoxy samples.

References

1. Maksimov, R. D.; Mochalov, V. P.; Urzhumtsev, Yu. S. *Polym Mech* 1972, 8, 685.
2. Onogi, S.; Sasaguri, K.; Adachi, T.; Ogihara, S. *J Polym Sci* 1962, 58, 1.
3. Emri, I.; Pavsek, V. *Mater Forum* 1992, 16, 123.
4. Fujita, H.; Kshimoto, A. *J Polym Sci* 1958, 28, 547.
5. Ishisaka, A.; Kawagoe, M.; Miyano, Y. *J Jpn Soc Mech Eng, A* 2002, 68, 611.
6. Fukumoto, O. *Polyamide Resin Handbook*; Nikkan Kougyo Shinbunsha: Tokyo, 1988; pp. 67–108 (in Japanese).
7. Miller, R. L. in *Polymer Handbook*; Brandrup, J.; Immergut, E. H., Eds.; Wiley-Interscience: New York, 1975; pp. III-25.
8. *JIS Hand Book Plastic*; Japan Standards Assoc: Tokyo, 1992; pp. 331–335.
9. *Koubunshigakkai'Zairyuu To Suibun Handbook*; Kyoritu Shuppan: Tokyo, 1968; pp. 239–260 (in Japanese).
10. Crank, J. *The Mathematics of Diffusion*, 2nd ed.; Oxford Univ. Press: Oxford, 1975; pp. 244–246.
11. Starkweather, H. W., Jr. *ACS Symp Ser* 1980, 127, 433.
12. Shinbo, M. *Epoxy Resin Handbook*; Nikkan Kougyo Shinbunsha: Tokyo, 1993; pp. 355–390 (in Japanese).
13. Ho, T.-H.; Wang, C. S. *Eur Polym J* 2001, 37, 267.
14. Chateauminois, A.; Chabert, B.; Soulier, J. P.; Vincent, L. *Polym Comp* 1995, 16, 288.
15. Akay, M.; Kong Ah Mun, S.; Stanly, A. *Comp Sci Technol* 1997, 57, 565.
16. Halpin, J. C. in *Composite Materials Workshop*; Tsai, S. W.; Halpin, J. C.; Pagano, N. J., Eds.; Technomic: Lancaster, PA, 1968; pp. 87–152.